Nat Hazards (2013) 65:1913–1930
DOI 10.1007/s11069-012-0454-4

ORIGINAL PAPER

Changes in annual and seasonal temperature extremes in the arid region of China, 1960–2010

Huaijun Wang · Yaning Chen · Zhongshen Chen · Weihong Li

Received: 19 July 2012 / Accepted: 9 October 2012 / Published online: 20 October 2012

Abstract Daily data of minimum and maximum temperature from 76 meteorological stations for 1960–2010 are used to detect the annual and seasonal variations of temperature extremes in the arid region, China. The Mann–Kendall test and Sen estimator are used to assess the significance of the trend and amount of change, respectively. Fifteen temperature indices are examined. The temperature extremes show patterns consistent with warming, with a large proportion of stations showing statistically significant trends. Warming trends in indices derived from daily minimum temperature are of greater magnitudes than those from maximum temperature, and stations along the Tianshan Mountains have larger trend magnitudes. The decreases in frequency for cold extremes mainly occur in summer and autumn, while warm extremes show significant increases in frequency in autumn and winter. For the arid region as a whole, the occurrence of cold nights and cold days has decreased by −1.89 and −0.89 days/decade, respectively, and warm nights and warm days has increased by 2.85 and 1.37 days/decade, respectively. The number of frost days and ice days exhibit significant decreasing trends at the rates of −3.84 and −2.07 days/decade. The threshold indices also show statistically significant increasing trends, with the extreme lowest temperatures faster than highest temperatures. The diurnal temperature range has decreased by 0.23 °C/decade, which is in accordance with the more rapid increases in minimum temperature than in maximum temperature. The results of this study will be useful for local human mitigation to alterations in water resources and ecological environment in the arid region of China due to the changes of temperature extremes.

H. Wang · Y. Chen (✉) · Z. Chen · W. Li
State Key Laboratory of Desert and Oasis Ecology, Xinjiang Institute of Ecology and Geography, Chinese Academy of Sciences (CAS), Urumqi, Xinjiang 830011, China
e-mail: chenyn@ms.xjb.ac.cn

H. Wang
The Graduate School of Chinese Academy of Sciences, Beijing 10049, China

Keywords Temperature extremes · Mann–Kendall test · Sen's slope estimates · The arid region

1 Introduction

In recent years, there is an increasing concern in weather and climate extremes, since they may cause serious disasters to human society and nature and seem to be more sensitive to climate change than mean values (Aguilar et al. 2009; Karl and Easterling 1999; Trigo et al. 2006). Many results have shown that the increases in economic losses, coupled with a rise in deaths, may be caused due to the facts that climate extremes are increasing in frequency and intensity. For example, heat waves occurred in summer of 2003 resulting in over 22,000 heat-related deaths across Europe (Schar and Jendritzky 2004); the unprecedented freezing disaster in January in South China caused great losses in the national economy, especially in almost countrywide transportation, energy supply, electric power transition, communication facilities, agricultural and ecological systems, and people's life (Ding et al. 2008). In China, cold waves break out over North China in winter frequently, while hot days and heat waves are commonly seen in South China in summer, and arid and semiarid regions in Northwest China often suffer from drought (Wang et al. 2011). Furthermore, changes in extremes can be strong indicators of climate change as it has been hypothesized that in a warming world where the atmosphere can hold more water vapor, the hydrological cycle could become more active (Aguilar et al. 2005). However, knowledge of changes in extremes compared with mean temperature is usually sparse, especially in the arid region of China which has the most fragile ecological environments in the world.

Temperature extremes have been studied in many regions, such as in Italy (Toreti and Desiato, 2008), Uruguay (Rusticucci and Renom 2008), South America (Vincent et al. 2005), Southern and Western Africa (New et al. 2006), Greece (Kioutsioukis et al. 2010), and also the global change (Alexander et al. 2007; Frich et al. 2002). These studies concluded that widespread significant change in temperature extremes is associated with warming especially for those indices derived from daily minimum temperature. Recent studies on the changes of temperature extremes over China suggested decreasing trends in cold extremes but increasing trends in warm extremes (Wang et al. 2011; You et al. 2011). Water is the foundation of composition, development, and stability of oasis ecosystems in arid areas and determines the evolution of the ecological environment (Chen et al. 2007). Temperature, especially in arid and semiarid areas, directly impacts the spatial and temporal distribution of water resources, because increasing temperature will severely influence the mountain glacier and then affect water supplies to rivers (Zhang et al. 2009). In China, recession of the mountain glaciers will threat to disrupt the water supply for people living in the arid area. Shi et al. (2007) indicated the climate in Northwest China started to change from warm-dry to warm-wet in the year of 1987, implying that temperature changes may alter hydrological cycle. Therefore, exploring changing characteristics of extreme temperature in the arid region of China is a prerequisite for the assessment of impacts of climatic changes on regional ecological environment and agricultural development.

This work is aimed at describing variations of temperature extremes under the rapid warming in recent five decades over the arid region of China. The paper is organized as follows. Section 2 describes the study area, data sets, and the methods used in this study. The spatial annual and seasonal trend distribution of temperature extremes are separately presented in Sect. 3. Discussions and conclusions are given in Sect. 4.

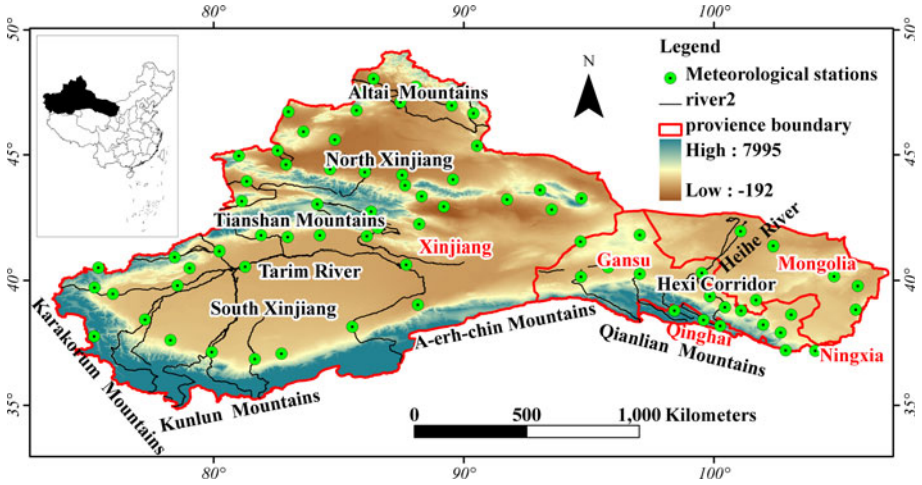

Fig. 1 Location of study region, main geographical features, and gauge stations in arid region of Northwest China

2 Study area, data, and methods

2.1 Study area

The arid region of China (Fig. 1) is distributed in the northwestern part of China ranging from 34 to 50 N and from 73 to 108 E including the provinces of Xinjiang, Gansu, western part of Inner Mongolia, and northern part of Ningxia and Qinghai. The arid region of Northwest China has rich land and mineral resources and plays an important role in China's future economic and social development. The arid region is located in inner center of Eurasia, being one of the most sensitive areas to global climate change. The arid region borders eight nations in Asia: Mongolia and Russia in the north, Kazakhstan, Kyrgyzstan, Tajikistan, and Afghanistan in the west, and Pakistan and India in the south. China's northwestern arid endorheic drainage basins cover a considerable area of 2.53 million km^2. These basins lie west of Helanshan Mountains in the Ningxia Hui Autonomous Region, and west of Ushaoling Mountains in Gansu Province. There are many endorheic drainage basins including the Tarim Basin, Tsaidam Basin, Badanjilin Desert, Tengger Desert, and other endorheic drainage basins in northern Xinjiang Uygur Autonomous Regions, the Alashangqi Desert in western Inner Mongolia, and Hexi Corridor Gobi Desert in Gansu Province. The climate of the arid region is typical of inner-continental land masses, with a wide temperature range, low precipitation, low humidity and lesser effects of East Asian Monsoon. The landscape of the region is characterized by a unique morphological complexity consisting of mountains, basins, and rivers and generates the lots of diverse biomes, which include forests, grasslands, deserts, and oases. The high vegetation coverage area mainly is composed of temperate coniferous forests, temperate grassland, sparse shrub steppe, and temperate and subtropical alpine meadow. The middle coverage area is composed of alpine cushion-like dwarf subshrub, subshrub steppe, one crop per annum, and cold-tolerant economic crop food. Vegetation types of low coverage area are subarbor, subshrub, and desert areas without vegetation. High coverage area is mainly concentrated in Altai Mountains, Tianshan Mountains, Qilian Mountains, and Mazongshan Mountains. Low coverage area is mainly concentrated in the

Tarim Basin, the Gashun Gobi, and central Gobi. The middle coverage area is composed of grasslands between high coverage areas and low coverage areas and regions of one crop per annum. The vegetation coverage in the northwest region appeared a clear seasonal variation. The vegetation coverage reached its maximum in July and August with the rising temperature and increasing precipitation (Zhang et al. 2010).

2.2 Data

A data set of daily minimum and maximum surface air temperature at 84 meteorological observing stations is used in this study. This data set is developed by the Climate Data Center (CDC) of the National Meteorological Center of the China Meteorological Administration (CMA) and has gone through the quality control procedures of the CDC. Stations that were installed after 1960 were excluded. About the data gap, monthly indices are calculated if no more than three days are missing in the month, and annual values if no more than 15 days are missing in the year. However, an annual value will also not be calculated if any month's data are missing. The procedures of RclimDex and Rhtest (available for download from http://cccma.seos.uvic.ca/ETCCDMI) are used to execute the quality controls (including identify error, search for outliers, assess homogeneity). As a result, 76 weather stations for 51 years (January 1, 1960, to February 28, 2011) are selected.

2.3 Methods

Data are analyzed using the RclimDex package (soft and documentation available for download from http://cccma.seos.uvic.ca/ETCCDMI), which can calculate 16 temperature extremes based on daily maximum and minimum temperature. In this paper, we only select 15 indices for analysis (Table 1). This paper also analyses seasonal values (ANN for annual change, DJF for winter, MAM for spring, JJA and SON for summer and autumn, respectively) of some indices, such as the absolute indices (TNn, TNx, TXn, TXx), the percentile temperature indices (TN10p, TN90p, TX10p, TX90p), and DTR whenever possible. This has been made possible because RClimDex also provides monthly values for these indices. The regionally averaged variations of temperature extremes are evaluated and tested for the whole arid region. Regional averages are calculated as an arithmetic mean of values at all stations in the study.

Some of the indices data do not have a Gaussian distribution, and in these cases, a simple linear least squares estimation would not be appropriate. Therefore, we use a nonparametric Kendall's tau-based slope estimator (Sen 1968), but statistical significance for the trends in extreme climate indices is performed using Mann–Kendall test (Kendall 1975; Mann 1945). A trend is considered to be statistically significant if it is significant at the 5 % level. The results of the M–K test are heavily affected by serial correlation of the time serial correlation on M–K results, and we adopt the Yue and Pilon method by using R package "ZYP" to remove lag-1 autocorrelation (Yue et al. 2002).

3 Results

3.1 Cold extremes (FD0, ID0, TN10p, TX10p, TNn, TXn, CSDI)

3.1.1 Annual changes

Figure 2 illustrates the spatial distributions of trends in annual cold extremes in recent five decades, and Fig. 3 demonstrates the regional annual and seasonal trends for all the indices

Table 1 Definitions of 15 temperature indices used in this study, and all the indices are calculated by RClimDEX

ID	Indicator name	Definitions	Units
Cold extremes			
FD0	Frost days	Annual count when TN(daily minimum) < 0 °C	Days
ID0	Ice days	Annual count when TX(daily maximum) < 0 °C	Days
TN10p	Cool nights	Percentage of days when TN < 10th percentile	Days
TX10p	Cool days	Percentage of days when TX < 10th percentile	Days
TNn	Coldest nights	Monthly minimum value of daily minimum temp	°C
TXn	Coldest days	Monthly minimum value of daily maximum temp	°C
CSDI	Cold spell duration indicator	Annual count of days with at least 6 consecutive days when TN < 10th percentile	Days
Warm extremes			
TN90p	Warm nights	Percentage of days when TN > 90th percentile	Days
TX90p	Warm days	Percentage of days when TX > 90th percentile	Days
TNx	Warmest nights	Monthly maximum value of daily minimum temp	°C
TXx	Warmest days	Monthly maximum value of daily maximum temp	°C
SU25	Summer days	Annual count when TX(daily maximum) > 25 °C	Days
TR20	Tropical nights	Annual count when TN(daily minimum) > 20 °C	Days
WSDI	Warm spell duration indicator	Annual count of days with at least 6 consecutive days when TX > 90th percentile	Days
Variability extremes			
DTR	Diurnal temperature range	Monthly mean difference between TX and TN	°C

in the arid region of China during 1960–2010. Table 2 shows the proportion of stations with negative, insignificant, and positive trends for yearly temperature extremes. For cold nights (TN10) and cold days (TX10), about 96 and 61.8 % of stations have decreasing trends that are statistically significant. Stations in Xinjiang, especially along the Tianshan Mountains, have larger trend magnitudes. The regional trend magnitudes for these two indices are −1.89 and −0.89 days/decade. Similarly, the temperature of coldest nights (TNn) and coldest days (TXn) have also statistically significant increased at approximately 60 and 89 % of stations, respectively. Stations situated in northern and central Xinjiang (along Tianshan) show the largest changes, and the regional trend magnitudes in TNn and TXn are 0.65 and 0.36 °C/decade, respectively. The number of frost days (FD0) has generally decreased with 90 % of stations showing a significant decrease at the 0.05 level. Stations with larger trend magnitudes are again distributed in central Xinjiang (along Tianshan). Ice days (ID0) has also decreased with 38 % of stations showing a significant decrease, and stations in the Qilian Mountains (southeastern arid areas) seem to show more statistically significant change. The number of days for FD0 and ID0 has averagely decreased by −3.84 and −2.07 days/decade, respectively. The number of cold spell duration indicator (CSDI) (not shown for distribution) has decreased at a rate of −0.66 days/decade, and about 99 % of stations show increasing trends but only 20 % of stations showing significant. As shown in Fig. 4, there are slow decreases in FD0, TN10p, and TX10p between 1960 and 1986 and then drastic decline with −6.8 days/decade, −1.53 days/decade, and −1.11 days/decade, respectively. For other cold extremes (ID0, TNn, TXn, CSDI), step change point is probably observed in 1986. The average is

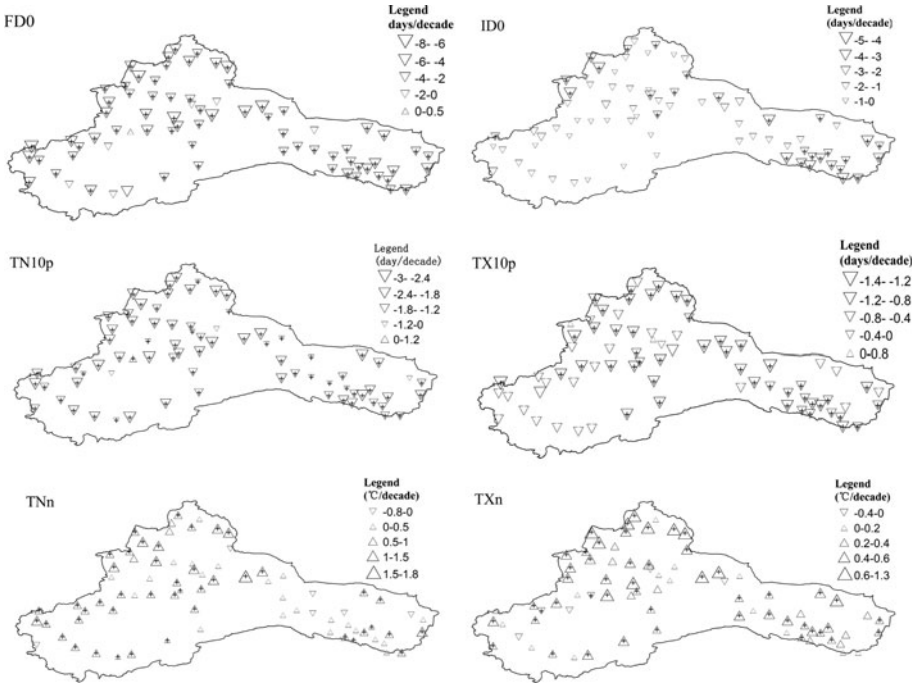

Fig. 2 Spatial patterns of trends per decade during 1960–2010 in the arid region of China of cold extremes (FD0, ID0, TN10p, TX10p, TNn, and TXn). Upward-pointing (downward pointing) *triangles* indicate increasing (decreasing) trends. *Triangles* with plus sign (+) and no symbol are significant at a 5 % level of significance and show no significant trend, respectively. The size of the triangles is proportional to the magnitudes of the trends

68.55 days, −26.07, −13.89 °C, and 4.68 days before 1986, whereas it changed to 61.19 days, −24.27, −12.58 °C, and 2.22 days after 1986 for ID0, TNn, TXn, and CSDI, respectively.

Table 3 shows the proportion of stations where trends in indices are of a particular relative magnitudes. About 96 % of stations show larger trend magnitudes in TN10 than in TX10. For TXn and TNn, 83 % of stations have greater trend magnitudes in TNn. About 79 % of stations show larger trend magnitudes in FD0 than ID0. For cold extremes, the minimum temperature extremes in the arid region of China have larger change than the maximum temperature extremes.

3.1.2 Seasonal changes

Figure 5 displays the seasonal variations of the occurrence frequency of cold nights (TN10p) in recent five decades over the arid region of China. Table 4 shows the percentage of stations with negative, insignificant, and positive trends for seasonal temperature extremes. It is apparent that the greatest contribution to the frequency of cold extremes is from SON (Fig. 3). For instance, coldest nights (TNn) have increased by 0.83 days/decade in autumn for the regional arid region, far more than the increase in any other season. We also see increases in the seasonal occurrence of coldest days (TXn) (Fig. 3; Table 4) are generally insignificant (apart from JJA). However, the number of stations showing more

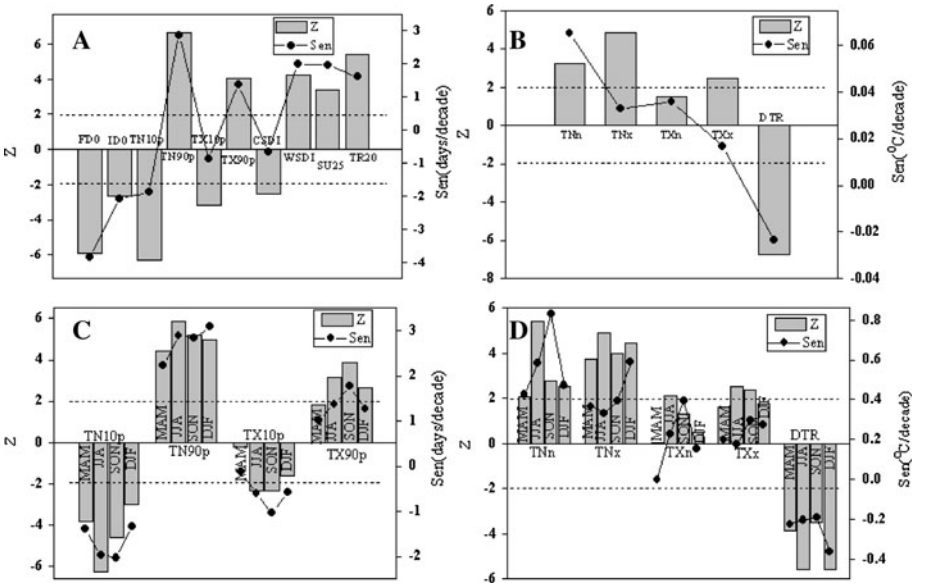

Fig. 3 Regional annual and seasonal trends for temperature indices. The *dot line* is the 95 % confidence level for Mann–Kendall test (A,B: annual change; C,D: seasonal change)

statistically significant trend is likely to occur in JJA. Taking cold nights (TN10p) (Fig. 5), for example, in MAM, JJA, SON, and DJF, significant decreasing trends are observed at 34, 84, 53, and 40 % of stations, respectively.

Table 3 shows the annual and seasonal proportion of stations where trends in indices are of a particular relative magnitude. About 91 % of stations show larger trend magnitudes in TNn than TXn in JJA, but it falls to 79 % in DJF. For TN10p versus TX90p, over 90 % of stations have greater trend magnitudes in TN10p for all four seasons.

3.2 Warm extremes (TN90p, TX90p, TNx, TXx, SU25, TR20, WSDI)

3.2.1 Annual changes

Changes in warm extremes during 1960–2010 are shown in Fig. 6. Figure 3 demonstrates the regional trends for warm extremes. The number of stations with negative, insignificant, and positive trends is listed in Table 2. For warm nights (TN90) and warm days (TX90), change to 96 and 92 % of stations shows statistically significant trends, respectively. Stations in central Xinjiang for TN90 and stations in southern Xinjiang and western Hexi Corridor for TX90 have larger trend magnitudes. The regional trend magnitudes for these two indices are 2.85 and 1.37 days/decade, respectively. The temperatures of the warmest days (TXx) and warmest nights (TNx) have also showed increases, but the spatial patterning is less consistent than for other indices, particularly for TXx. About 62 % of stations, mainly in Northern Xinjiang, show significant increases in TNx, but only 29 % of stations for TXx show statistically significant trends. For TNx and TXx, the regional trend magnitudes also show statistically increasing trend with the rate equivalent to 0.33 and 0.17 °C/decade. For the summer days (SU25) and tropical nights (TR20), about 53 and 46 % of stations show statistically significant increase, and the regional trend magnitudes

Table 2 Percentage of stations showing significant annual trends for each index

	TN10p	TN90p	TX10p	TX90p	TNn	TNx	TXn	TXx	DTR	FD0	ID0	CSDI	SU25	TR20	WSDI
SP	1.3	96.1	0	91.8	59.2	61.8	88.2	28.9	2.63	0	0	0	69.7	60.5	69.7
ISP	0	1.3	1.3	8.2	32.9	31.6	10.5	55.3	7.9	1.3	1.3	1.3	21.1	9.2	28.9
ISN	2.6	1.3	36.8	0	7.9	3.9	1.3	11.8	14.5	9.2	60.5	78.9	1.3	5.3	1.3
SN	96.1	1.3	61.8	0	0	2.6	0	2.63	75	89.5	38.2	19.7	2.6	2.6	0

SP significant positive trend, *ISP* insignificant positive trend, *ISN* insignificant negative trend, *SN* significant negative trend

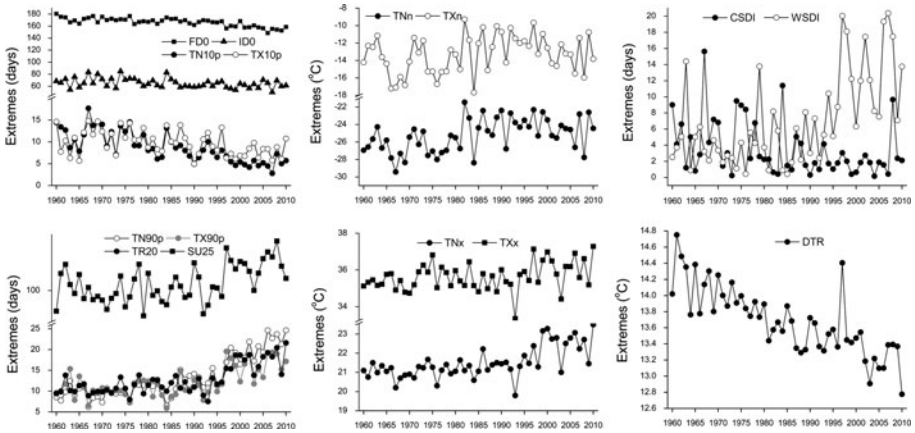

Fig. 4 Regional time series of temperature extremes

Table 3 Proportion of individual stations where the trend in one index is of greater magnitudes than the trend in a second

Index	Comparison	Proportion				
		ANN	MAM	JJA	SON	DJF
TX90 > TX10	abs	0.89	0.87	0.89	0.84	0.99
TN90 > TN10	abs	0.89	0.87	0.79	0.66	0.96
TXn > TXx	rel	0.78	0.26	0.70	0.57	0.34
TNn > TNx	rel	0.74	0.58	0.86	0.91	0.36
TNx > TXx	rel	0.78	0.79	0.76	0.46	0.88
TNn > TXn	rel	0.83	0.91	0.86	0.83	0.79
FD0 > ID0	abs	0.79				
TN90 > TX90	abs	0.87	0.86	0.83	0.66	0.91
TN10 > TX90	abs	0.71	0.63	0.67	0.55	0.51
TN10 > TX10	abs	0.96	0.92	0.95	0.96	0.93
TN90 > TX10	abs	0.97	0.96	0.95	0.89	0.99

abs, the absolute magnitudes of trends are compared; rel the signs of trends are retained during comparison

for those are 1.96 and 1.59 days/decade, respectively. Warm spell duration indicator (WSDI) (not shown for distribution) have also increased, with a regional averaged increase of 1.97 days/decade; stations showing significant trends are distributed in southern Xinjiang and western Hexi corridor. The step change for annual warm extremes was identified as occurred in 1995. The average before 1995 is 4.06, 9.73, 10.17, 10.94, 99.88 days, 21.10 and 35.51 °C for WSDI, TN90p, TX90p, TR20, SU25, TNx and TXx (Fig. 4), respectively, while that after 1995 is 10.45, 17.42, 14.33, 14.84, 104.99 days, 21.98 and 35.80 °C.

Table 3 again shows comparative trends at individual sites. Compared with TX90, about 87 % of stations have greater trend magnitudes in TN90, and approximately 78 % of stations have greater trend magnitudes in TNx than in TXx.

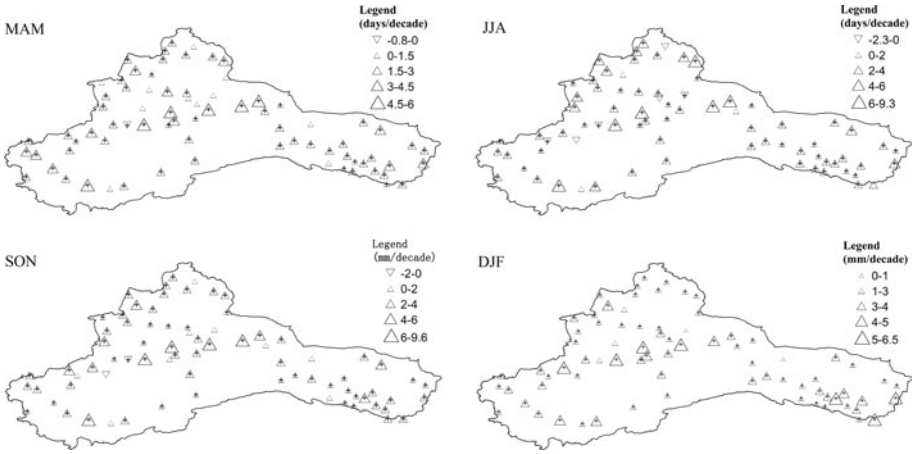

Fig. 5 As Fig. 2 but for the seasonal occurrence of cold nights (TN10p)

3.2.2 Seasonal changes

The spatial distribution of seasonal trend magnitudes of warm nights (TN90p) is shown in Fig. 7. Table 4 shows the number of stations with negative, insignificant, and positive trends for seasonal temperature extremes. In a majority of cases, seasonal warm extremes suggest increasing trends. For the indices of TN90p and TNx, the regional trends in DJF, with the trend magnitudes of 3.01 days/decade and 0.59 °C/decade, respectively, show the largest trend magnitudes compared with other season. For TX10p and TXx, SON is the season showing the largest regional trend magnitudes. The patterns of number of stations showing most statistically significant trend are likely to the regional trend. For TN90p, TNx, TX90p, and TXx, the largest proportion of stations with positive seasonal trends is 93 % (DJF), 76 % (DJF), 84 % (SON), and 46 % (SON), respectively.

Table 3 shows comparative trends at individual sites for seasonal scale. Compared with TX90 in DJF, about 91 % of stations have greater magnitudes in TN90p and the proportion decline to 86, 83, and 66 % in MAM, JJA, and SON, respectively. Approximately 88 % of stations show larger trend magnitudes in TNx than in TXx for the season of DJF; the percentage of stations declines to 79 % in MAM, 76 % in JJA, and 46 % in DJF, respectively.

3.3 Comparison of warm and cold extremes

In order to learn more about the relative changes in the daily temperature distribution, it is necessary to compare trends in warm and cold indices, and the results are shown in Table 3. For TX90 versus TX10, about 89 % of stations have larger trend magnitudes in TX90, and this proportion reaches 99 % in DJF; the regional trend in TX90 (1.37 days/decade) is slightly more than 1.5 times than that of TX10 (−0.89 days/decade). For TN90 versus TN10, the regional trend in TN90 (2.85 days/decade) is of greater magnitude than that of TN10 (−1.89 days/decade), about 89 % of stations having higher trend magnitudes in TN90 than in TN10. In MAM, JJA, SON, and DJF, the larger trend magnitudes in TN90 than in TN10 are observed at 87, 79, 66, and 96 % of the total stations. For TXx and TXn, however, the regional trend in TXn (0.36 °C/decade) is much higher than in TXx

Table 4 Percentage of stations showing significant trends at the 5 % level for each season between 1960 and 2010 for indices that can be calculated seasonally

Indicator	MAM				JJA				SON				DJF			
	SP	ISP	ISN	SN	SP	ISP	ISN	SN	SP	ISP	ISN	SN	SP	ISP	ISN	SN
TN10p	1.3	3.9	25	69.7	0	6.6	5.3	88.2	1.3	1.3	10.5	86.8	1.3	3.9	32.8	61.8
TN90p	84.2	14.5	0	1.3	86.8	5.3	3.9	3.9	85.5	11.8	1.3	1.3	93.4	6.5	0	0
TX10p	0	18.4	84.5	1.3	2.6	9.2	57.9	30.2	1.3	1.3	64.4	32.9	0	10.5	82.9	6.6
TX90p	31.6	65.8	2.6	0	46.1	40.8	9.2	3.9	84.2	15.8	0	0	55.3	44.7	0	0
TNn	34.2	47.4	18.4	0	84.2	14.5	1.3	0	52.6	46.1	0	0	39.4	0.5	9.2	0
TNx	50	46.1	3.9	0	59.2	31.6	6.6	2.6	52.6	44.7	1.3	1.3	76.3	23.7	0	0
TXn	2.6	42.1	55.3	0	13.2	77.6	9.2	0	1.3	97.4	1.3	0	3.9	71.1	0.25	0
TXx	18.4	76.3	3.9	1.3	27.6	55.3	11.8	5.3	46.1	52.6	1.3	0	19.7	67.1	14.5	0
DTR	1.3	3.9	40.8	53.9	9.2	3.9	26.3	60.5	5.3	22.4	0.25	47.4	2.6	7.9	21.1	68.4

SP significant positive trend, *ISP* insignificant positive trend, *ISN* insignificant negative trend, *SN* significant negative trend

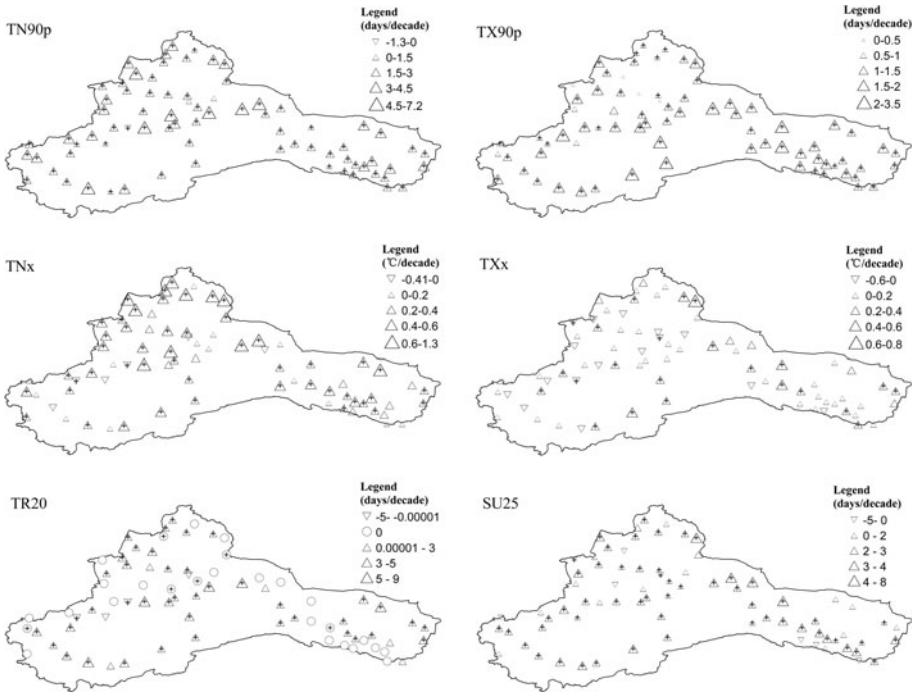

Fig. 6 As Fig. 2 but for the warm extremes

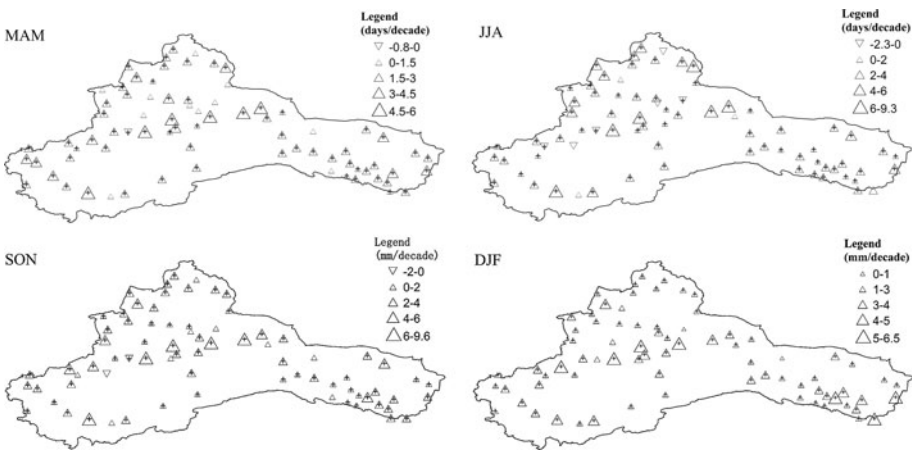

Fig. 7 As Fig. 2 but for the seasonal TN90

(0.17 °C/decade), and roughly, 78 % of stations show larger trends in TXn. The magnitude of the regional trends in TNn (0.65 °C/decade) is more than two times than that of TNx (0.33 °C/decade). At individual stations, about 74 % of stations have greater trend magnitudes in TNn compared with TNx. Therefore, we can conclude that changes in

percentile-based warm extremes (TN90 and TX90) seem to be larger than changes in percentile-based cold extremes with the largest change in DJF, while absolute-based warm extremes (TNx and TXx) seem to have smaller trend magnitudes than in absolute-based cold extremes (TNn and TXn), which is in agreement with the results of eastern and central Tibetan (You et al. 2008). By the preceding analysis, we also can see changes in extremes derived from daily minimum temperature (TN10, TN90, TNn, TNx) are generally larger than changes in extremes derived from daily maximum temperature (TX10, TX90, TXn, TXx, respectively).

3.4 DTR

For annual DTR, about 75 % of stations show a significant decreasing trend in the arid region of China (Table 2). Stations in the Xinjiang area have larger trend magnitudes. A few stations showing significant decrease mainly occur in the eastern arid region (Fig. 8). The regional trend magnitude in DTR is −0.23 °C/decade, retaining the clearing decreasing trend throughout the whole period. The trend for DTR varies throughout the seasons, highlighting the importance of examining each season rather than just the annual average. Stations with larger trend magnitudes again distribute along the Tianshan Mountains especially for the season of DJF. DJF has the most widespread significant change with the regional trend magnitude of −0.37 °C/decade. Significance test results (Table 4) indicate that 54, 61, 47, and 68 % of stations in MAM, JJA, SON, and DJF show significant decrease in trends, respectively. The decrease in DTR might be mainly caused by a faster increase in minimum temperature than in maximum temperature, which

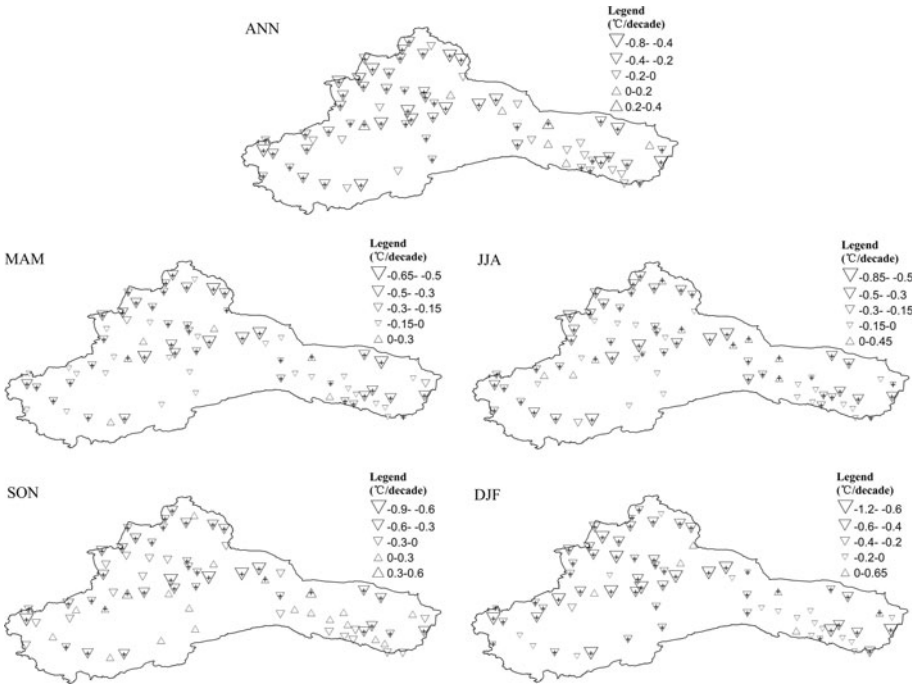

Fig. 8 As Fig. 2 but for the annual and seasonal diurnal temperature range (DTR)

indicates a warming trend in the climate (Liu et al. 2009). The decrease in DTR might be mainly due to the increase in vapor and aerosol in the air, which reduces the daytime incoming solar radiation and also the nighttime outgoing longwave radiation from the land surface, resulting in a high minimum temperature (Shen et al. 2010).

4 Discussion and conclusions

Observed trends in annual and seasonal temperature extremes in the arid region of China were thoroughly analyzed by using daily maximum and minimum temperatures for 76 stations. Some interesting conclusions can be drawn as follows:

1. Between 1960 and 2010, over 96 % of stations show a significant decrease in the annual occurrence of cold nights (TN10p), while the occurrence of warm nights (TN90p) shows a similar proportion of significant increase. For other indices, the majority of the temperature extremes exhibit a statistically significant change, especially for the indices of cold days (TX90p), coldest days (TXn), and frost days (FD0) with the proportion all more than 85 %. Stations along the Tianshan Mountains have larger positive trends in warm extremes and negative trends in cold extremes. Glacier runoff is the major contributor to water resources that are used to support the sustainable development of the environment, industry, and agriculture in arid regions (Yao et al. 2004). With climatic warming, glaciers, especially the smaller glaciers, are at risk of being strongly impacted. It is predicted that the smaller glaciers (area < 1 km^2) on the northern slope of the Chinese Tianshan Mountains will likely disappear within the next 20–40 years (Li et al. 2010). Extremes derived from daily minimum temperature (TN10 and TN90) are generally larger than changes in extremes derived from daily maximum temperature (TX10 and TX90), and changes in minimum of daily minimum and maximum temperature (TNn and TXn) generally have higher trend magnitudes than that in maximum of daily minimum and maximum temperature (TNx and TXx), which consist in a long-term decrease in DTR. In general, the changes in temperature extremes documented here are what the arid region of China expects in a warming world: decreases in cold extremes (FD0, ID0, TN10p, and TX10p) and increases in warm extremes (TN90p, TX90p, TXx, TNx). Besides, decreases in extremes derived from minimum temperatures are greater than the increases in extremes derived from maximum temperature. Compared with other regions in the world (Alexander et al. 2006; Zhang et al. 2005; New et al. 2006; You et al. 2011), patterns in the arid region are broadly similar, but there are some differences. Changes in temperature extremes seem to be larger trend magnitudes than those of other regions; especially, for the DTR, the decrease in magnitudes is stronger in the arid of China than those reported in all other regions. The decline in the spatial component of the variance of the near-surface air temperature in worldwide is generally due to the northern pole warming faster than the equator; the decline in the temporal component of the variance of the near-surface air temperature is generally due to winter temperatures increasing faster than summer temperatures, particularly in cold regions such as the North China, Russia, and Greenland (Sun et al. 2010). So, the most significant signals in the air temperature record are the decrease in the diurnal temperature range over land, largely due to rising of the minimum temperatures. Internal dynamics of the stable nocturnal boundary layer may play in affecting the response and sensitivity of the minimum temperatures to added downward longwave

forcing (McNider et al. 2012). The stable nocturnal boundary layer is very sensitive to changes in greenhouse gas forcing, surface roughness, wind speed, and heat capacity (Walters et al. 2007). It is likely that part of the increase in minimum temperature is reflecting a redistribution of heat by changes in turbulence of heat in the boundary layer (McNider et al. 2012). In fact, shelter-level temperature in the stable nocturnal boundary layer is very sensitive to added radiation, and the temperature changes on the order of 0.3–0.6 K due to a radiative forcing of 4.8 W m^{-2} would account for 50 % of the trend in the instrumental record for the twentieth century. The warming climate change also may well be associated with rapid urbanization, increased aerosol loading, and/or other land-use change (You et al. 2011). Urban heat island effects were found separately accounting for about 40 and 80 % of the rising of surface air temperature in North China and Southeast China (Ren et al. 2008; Zhou et al. 2004). Although the Northwest China has experienced slower urbanization than the southeast, this effect also cannot be ignored. However, Parker (2004, 2006) found that the warming was not caused by the urban heat island effect due to a temperature perturbation that was largely independent of wind speed, and they also further concluded that the warming in the record must be due to greenhouse gas (GHG) increases. However, we have not assessed potential effects for urbanization bias in this paper, and further work is required to address this issue.

2. Seasonal warming is apparent in all seasons. For cold extremes, the greatest contribution to the frequency of cold extremes is from SON; however, JJA is the season with most of the stations showing statistically significant change. For warm extremes, the regional trends of TN90p and TNx in DJF show the largest magnitudes compared with other seasons; for TX90p and TXx, SON is the season showing the largest regional trend magnitudes. The seasonal patterns for number of stations showing most statistically significant trend are likely to the regional trends. The largest proportion of stations with positive seasonal trends is DJF for TN90p and TNx, and SON for TX90p and TXx, respectively. This is not in accordance with results of Wang et al. (2011), which pointed out that frequency decreases in cold extremes mainly occurred in winter and warm extremes displayed both remarkable frequency increases in winter and summer in China. The reason for this difference will be discussed in the next work.

In recent years, air temperature and precipitation in the arid region of Northwest China show upward tendency during the past several decades. Annual streamflow of many rivers showed an increasing trend in mountainous region. The increased rainfall will result in increasing runoff in the headwater of inland rivers. However, impacts of the increased air temperature on streamflow have shown different characteristics depending on location and seasons: It has positive effects on the runoff at mountainous region due to the snowmelt and glacier melt in spring, but negative effect on the runoff at plain area due to the increase in actual evaporation in summer (Xu et al. 2010). Warming climate has resulted in the glacier retreat and glacier melt water increased. Glacier area is reduced by 1,400 km^2 from 1960 to 1995, and the annual runoff of glacier melt water was 84.2 % higher in 1985–2001 than during 1958–1985 at Glacier No.1 of the Urumqi River, Tianshan (Shi et al. 2007). Located in inland and far from oceans, the arid region of Northwest China is well known for arid climate. The most serious natural disaster here is droughts characterized by the vast effected area, long duration, and occurred frequently. Although the arid region is famous for its extensive desert and little rainfall, the floods caused by glacier melting also occur here every year. Frequency of flood disasters largely increased with extraordinary flood

occurring seven times during 1956–1986 and 21 times during 1982–2000 in Xinjiang area (Shi et al. 2007). With the climate change, vegetation cover in the arid region of northwest of China have increased, especially in Xinjiang (Li et al. 2009). Over the past 22 years, about 30 % of the total vegetated area showed an annual increase of 0.7 % in growing season NDVI (Zhao et al. 2011). Life zone diversity in Xinjiang of Northwest China was the highest in the 1960s, dramatically decreased in the 1970s, and then gradually increased in the 1980s and 1990s, implying a more stable environment since the 1970s (Zheng et al. 2006; Ni 2011). However, eco-environmental problems, such as the degenerated natural vegetation, land desertification, and the increased weather disaster, also subsequently occurred in the some arid region of Northwest China (Hao et al. 2008). For example, with the streamflow decrease significantly in the mainstream, the Lop Nur, the Taitema Lake, and more than 320 km of the lower section at the lower reaches have dried up (Feng et al. 2005). Since the 1950s, the condition and diversity of vegetation in the Tarim River Basin have significantly declined, with forest biomass in the basin decreased about fivefold during the period of 1960–1990 and herbaceous species decreased from 200 to 20 and wild animals species decreased from 26 to 5 (Xu et al. 2010). Due to the high intensity of water resource utilization and climate change in the upper reach of the Tarim River, the desert riparian forest vegetation and biodiversity has been damaged heavily, making the "Green Passage" at the lower reach of the Tarim River between the Taklimakan Desert and the Kuruk Desert on the verge of disappearance.

This paper provides some interesting conclusions for the temperature extreme changes using the RclimDex package in the arid region of Northwest China. However, due to the complexity of the climatic system and the geographical environment in the arid region, it is difficult to understand the climatic process thoroughly. We hope that better physical mechanism investigation will be proposed to complement the insufficiency in our paper.

Acknowledgments The research is supported by the National Basic Research Program of China (973 Program: 2010CB951003). Assistance on data processing and paper writing from Yongbo LIU is greatly appreciated. The authors thank the National Climate Central, China Meteorological Administration, for providing the meteorological data for this study.

References

Aguilar E, Peterson TC, Obando PR, Frutos R, Retana JA, Solera M, Soley J, Garcia IG, Araujo RM, Santos AR, Valle VE, Brunet M, Aguilar L, Alvarez L, Bautista M, Castanon C, Herrera L, Ruano E, Sinay JJ, Sanchez E, Oviedo GIH, Obed F, Salgado JE, Vazquez JL, Baca M, Gutierrez M, Centella C, Espinosa J, Martinez D, Olmedo B, Espinoza CEO, Nunez R, Haylock M, Benavides H, Mayorga R (2005) Changes in precipitation and temperature extremes in Central America and northern South America, 1961–2003. J Geophys Res-Atmos 110 (D23). doi:10.1029/2005jd006119

Aguilar E, Barry AA, Brunet M, Ekang L, Fernandes A, Massoukina M, Mbah J, Mhanda A, do Nascimento DJ, Peterson TC, Umba OT, Tomou M, Zhang X (2009) Changes in temperature and precipitation extremes in western central Africa, Guinea Conakry, and Zimbabwe, 1955–2006. J Geophys Res-Atmos 114 (D02115). doi:10.1029/2008JD011010

Alexander LV, Zhang X, Peterson TC, Caesar J, Gleason B, Tank A, Haylock M, Collins D, Trewin B, Rahimzadeh F, Tagipour A, Kumar KR, Revadekar J, Griffiths G, Vincent L, Stephenson DB, Burn J, Aguilar E, Brunet M, Taylor M, New M, Zhai P, Rusticucci M, Vazquez-Aguirre JL (2006) Global observed changes in daily climate extremes of temperature and precipitation. J Geophys Res-Atmos 111(D5). doi:10.1029/2005jd006290

Alexander LV, Hope P, Collins D, Trewin B, Lynch A, Nicholls N (2007) Trends in Australia's climate means and extremes: a global context. Aust Meteorol Mag 56(1):1–18

Chen YN, Li WH, Xu CC, Hao XM (2007) Effects of climate change on water resources in Tarim River Basin, Northwest China. J Environ Sci-China 19(4):488–493

Ding YH, Wang ZY, Song YF, Zhang J (2008) The unprecedented freezing disaster in January 2008 in Southern China and its possible association with the global warming. Acta Meteorol Sin 22(4):538–558
Feng Q, Liu W, Si JH, Su YH, Zhang YW, Cang ZQ, Xi HY (2005) Environmental effects of water resource development and use in the Tarim River basin of northwestern China. Environ Geol 48(2):202–210. doi:10.1007/s00254-005-1288-0
Frich P, Alexander LV, Della-Marta P, Gleason B, Haylock M, Tank AMGK, Peterson T (2002) Observed coherent changes in climatic extremes during the second half of the twentieth century. Clim Res 19(3):193–212
Hao XM, Chen YN, Xu CC, Li WH (2008) Impacts of climate change and human activities on the surface runoff in the Tarim River basin over the last fifty years. Water Resour Manag 22(9):1159–1171. doi:10.1007/s11269-007-9218-4
Karl TR, Easterling DR (1999) Climate extremes: selected review and future research directions. Clim Change 42(1):309–325
Kendall MG (1975) Rank-correlation measures. Charles Griffin, London, p 202
Kioutsioukis I, Melas D, Zerefos C (2010) Statistical assessment of changes in climate extremes over Greece (1955–2002). Int J Climatol 30(11):1723–1737. doi:10.1002/joc.2030
Li XH, Shi QD, Guo J (2009) The response of NDVI to climate variability in Northwest Arid Area of China from 1981 to 2001. J Arid Land Resour Environ 23(2):12–16 (in Chinese)
Li ZQ, Li KM, Wang L (2010) Study on recent glacier changes and their impact on water resources in Xinjiang, Northwestern China. Q Sci 30(1):96–106 (in Chinese)
Liu M, Shen Y, Liu C (2009) Change trend of pan evaporation and its cause analysis over the past 50 years in China. Acta Geogr Sinica 64(3):259–269
Mann HB (1945) Non-parametric tests against trend. Econometrica 13:245–259
McNider RT, Steeneveld GJ, Holtslag AAM, Pielke RA, Mackaro S, Pour-Biazar A, Walters J, Nair U, Christy J (2012) Response and sensitivity of the nocturnal boundary layer over land to added longwave radiative forcing. J Geophys Res-Atmos 117. doi:10.1029/2012jd017578
New M, Hewitson B, Stephenson DB, Tsiga A, Kruger A, Manhique A, Gomez B, Coelho CAS, Masisi DN, Kululanga E, Mbambalala E, Adesina F, Saleh H, Kanyanga J, Adosi J, Bulane L, Fortunata L, Mdoka ML, Lajoie R (2006) Evidence of trends in daily climate extremes over southern and west Africa. J Geophys Res-Atmos 111(D14). doi:10.1029/2005jd006289
Ni J (2011) Impacts of climate change on Chinese ecosystems: key vulnerable regions and potential thresholds. Reg Environ Change 11:S49–S64. doi:10.1007/s10113-010-0170-0
Parker DE (2004) Climate—large-scale warming is not urban. Nature 432(7015):290. doi:10.1038/432290a
Parker DE (2006) A demonstration that large-scale warming is not urban. J Clim 19(12):2882–2895. doi:10.1175/jcli3730.1
Ren GY, Zhou YQ, Chu ZY, Zhou JX, Zhang AY, Guo J, Liu XF (2008) Urbanization effects on observed surface air temperature trends in north China. J Clim 21(6):1333–1348
Rusticucci M, Renom M (2008) Variability and trends in indices of quality-controlled daily temperature extremes in Uruguay. Int J Climatol 28(8):1083–1095. doi:10.1002/joc.1607
Schar C, Jendritzky G (2004) Climate change: hot news from summer 2003. Nature 432(7017):559–560
Sen PK (1968) Estimates of the regression coefficient based on Kendall's Tau. J Am Stat As 63:1379–1389
Shen YJ, Liu CM, Liu M, Zeng Y, Tian CY (2010) Change in pan evaporation over the past 50 years in the arid region of China. Hydrol Process 24(2):225–231. doi:10.1002/Hyp.7435
Shi YF, Shen YP, Kang E, Li DL, Ding YJ, Zhang GW, Hu RJ (2007) Recent and future climate change in northwest china. Clim Change 80(3–4):379–393. doi:10.1007/s10584-006-9121-7
Sun FB, Roderick ML, Farquhar GD, Lim WH, Zhang YQ, Bennett N, Roxburgh SH (2010) Partitioning the variance between space and time. Geophys Res Lett 37. doi:10.1029/2010gl043323
Toreti A, Desiato F (2008) Changes in temperature extremes over Italy in the last 44 years. Int J Climatol 28(6):733–745
Trigo R, Pereira J, Pereira M, Mota B, Calado M, DaCamara C, Santo F (2006) The exceptional fire season of summer 2003 in Portugal. Int J Climatol 26(13):1741–1757
Vincent LA, Peterson TC, Barros VR, Marino MB, Rusticucci M, Carrasco G, Ramirez E, Alves LM, Ambrizzi T, Berlato MA, Grimm AM, Marengo JA, Molion L, Moncunill DF, Rebello E, Anunciacao YMT, Quintana J, Santos JL, Baez J, Coronel G, Garcia J, Trebejo I, Bidegain M, Haylock MR, Karoly D (2005) Observed trends in indices of daily temperature extremes in South America 1960–2000. J Clim 18(23):5011–5023
Walters JT, McNider RT, Shi X, Norris WB, Christy JR (2007) Positive surface temperature feedback in the stable nocturnal boundary layer. Geophys Res Lett 34 (12). doi:10.1029/2007gl029505
Wang Y, Xu X, Du YG, Tang JP (2011) Variations of temperature and precipitation extremes in recent two decades over China. Atmos Res 101(1–2):143–154

Xu ZX, Liu ZF, Fu GB, Chen YN (2010) Trends of major hydroclimatic variables in the Tarim River basin during the past 50 years. J Arid Environ 74(2):256–267. doi:10.1016/j.jaridenv.2009.08.014

Yao TD, Wang YQ, Liu SY, Pu JC, Shen YP, Lu AX (2004) Recent glacial retreat in High Asia in China and its impact on water resource in Northwest China. Sci China Ser D-Earth Sci 47(12):1065–1075. doi:10.1360/03yd0256

You QL, Kang SC, Aguilar E, Yan YP (2008) Changes in daily climate extremes in the eastern and central Tibetan Plateau during 1961–2005. J Geophys Res-Atmos 113 (D7). doi:10.1029/2007jd009389

You QL, Kang SC, Aguilar E, Pepin N, Flugel WA, Yan YP, Xu YW, Zhang YJ, Huang J (2011) Changes in daily climate extremes in China and their connection to the large scale atmospheric circulation during 1961–2003. Clim Dyn 36(11–12):2399–2417. doi:10.1007/s00382-009-0735-0

Yue SP, Pilon B, Cavadias G (2002) The influence of autocorrelation on the ability to detect trend in hydrological series. Hydrol Process 16:1807–1829

Zhang XB, Aguilar E, Sensoy S, Melkonyan H, Tagiyeva U, Ahmed N, Kutaladze N, Rahimzadeh F, Taghipour A, Hantosh TH, Albert P, Semawi M, Ali MK, Al-Shabibi MHS, Al-Oulan Z, Zatari T, Khelet IA, Hamoud S, Sagir R, Demircan M, Eken M, Adiguzel M, Alexander L, Peterson TC, Wallis T (2005) Trends in Middle East climate extreme indices from 1950 to 2003. J Geophys Res-Atmos 110 (D22). doi:10.1029/2005JD006181

Zhang Q, Xu CY, Zhang ZX, Chen YD (2009) Changes of temperature extremes for 1960–2004 in Far-West China. Stoch Env Res Risk Assess 23(6):721–735. doi:10.1007/s00477-008-0252-4

Zhang CX, Wang XM, Guo J (2010) Effects of vegetation change on wind-sand activity in Northwestern China. J Desert Res 30(2):254–259 (in Chinese)

Zhao X, Tan K, Zhao S, Fang J (2011) Changing climate affects vegetation growth in the arid region of the northwestern China. J Arid Environ 75(10):946–952. doi:10.1016/j.jaridenv.2011.05.007

Zheng Y, Xie Z, Jiang L, Shimizu H, Drake S (2006) Changes in Holdridge life zone diversity in the Xinjiang Uygur Autonomous Region (XUAR) of China over the past 40 years. J Arid Environ 66(1):113–126. doi:10.1016/j.jaridenv.2005.09.005

Zhou LM, Dickinson RE, Tian YH, Fang JY, Li QX, Kaufmann RK, Tucker CJ, Myneni RB (2004) Evidence for a significant urbanization effect on climate in China. Proc Natl Acad Sci USA 101(26):9540–9544